Low Voltage CO2-Gas Sensor Based on III–V Mid-IR Immersion Lens Diode Optopairs: Where we Are and How Far we Can Go?

Galina Yu. Sotnikova, Gennadyy A. Gavrilov, Sergey E. Aleksandrov, Alexander A. Kapralov, Sergey A. Karandashev, Boris A. Matveev, and Maxim A. Remennyy

***Abstract*—This study presents a comparative analysis of parameters of infrared radiation source and detector hardware that are most important for the creation of portable optical nondispersive infrared (NDIR) gas sensors. An analytical model of the optical gas sensor is proposed. The notions of an instrument and transfer functions of the sensor as a measurement device are introduced. Capabilities of the model have been demonstrated by the example of carbon dioxide sensor based on immersion diode optopairs. Validity of the model is proved by good coincidence of calculated and experimental data. Analytical description of the transfer function of a NDIR carbon dioxide sensor allowed us to carry out the comparative analysis of potential sensitivity of sensors based on different hardware produced by basic fabricators of IR components.**

***Index Terms*—Gas sensor transfer function, immersion diode optopairs, nondispersion infrared (NDIR) gas sensor, sensor instrument function.**

I. Introduction

NONDISPERSIVE optical methods of detection and measurement of gas concentration within the spectrum range 3–5 μm (mid IR) are generally implemented in gas analyzers that refer to a portable device class. The optical methods of gas analysis are superior in their capabilities to electrical chemical and catalytical ones used in this device class by ensuring high operation speed, selectivity, corrosive medium stability, service long life.

In the first place, the progress in optical nondispersive devices of gas spectral analysis is related to the development of IR sensors with a new and more efficient hardware, which includes, first of all, immersion lens light-emitting diodes and photodiodes [1], [2].

The immersion lens diodes that have been developed at Ioffe Physical-Technical Institute of the Russian Academy of Sciences represent a "flip-chip" design, where efficient immersion matching with microlenses is performed by using a chalcogenide glass ("glue") with a high refractive index ($n = 2.4$–2.8). New technical process of fabrication of light-emitting diodes allowed obtaining a considerable (two to threefold) increase of emergent radiation in semiconductor structures and radiation power up to 120 μW in a pulse mode at $\lambda = 4.2$ μm [3]. The detectability of immersion photodiodes is higher than that of devices fabricated with using conventional techniques, too, and it reaches the values $10^{10} - 10^{11}$ cm Hz$^{1/2}$/W at $\lambda = 3 - 4$ μm [4].

The technological know-how permits the fabrication of optopairs (spectrum-matched light-emitting diodes and photodiodes) in the range 3–5 μm with a sufficiently narrow spectral bandwidth (FWHW $\sim 0.1\lambda$), matched to absorption line spectra of a material under study and narrow angle of emittance/view (FWHW $\leq 40^\circ$), which allows one to use them in nondispersive spectral analysis instrumentation without additional spectral filters.

Recently, several EC projects aiming at optical gas sensor development have been launched [5]. Therefore, taking into account the fact that new types of optical sensors are of great interest to gas analysis equipment engineers, we have stated a problem to carry out the comparison of the present hardware of IR radiation sources and detectors from the point-of-view of their potential use in nondispersion infrared (NDIR) gas sensors and to develop a computative instrument (analytical model) for estimating their potential parameters.

We have suggested [6] to carry out the measurement techniques consideration of a NDIR gas sensor by describing its performance with an instrument and transfer functions. This approach together with the analysis of the noise and frequency characteristics of electronic circuits of signal detection permits one to calculate parameters which are important for estimating the quality of measurement devices: threshold sensitivity (limit of detection, LOD) and absolute and relative measurement errors (sensitivity and accuracy) within a wide range of concentrations of a gas under study.

This study presents the analytical model of the NDIR CO_2 sensor based on immersion lens diode optopairs. In order to develop this model it was necessary to obtain an analytical description of CO_2 absorption spectrum and spectral characteristics of immersion light-emitting diodes and photodiodes. A set of experimental studies with using a laboratory model of a miniature CO_2 sensor has been carried out to prove the efficiency of the analytical model.

Manuscript received April 02, 2009; revised August 06, 2009; accepted September 15, 2009. This work was supported in part by The Foundation for Assistance to Small Innovative Enterprises (FASIE) under GK 4269p/4719 and in part by a grant from the Seventh Frame Program of EC (FP7, No 224625). This is an expanded paper from the IEEE SENSORS 2008 Conference. The associate editor coordinating the review of this paper and approving it for publication was Dr. Krikor Ozanyan.

The authors are with the Ioffe Physical-Technical Institute, St. Petersburg, 194021, Russia (e-mail: gga_holo@mail.ru; infracell@mail.ru; sergey218@mail.ru; kapr_alex@mail.ru; ksa08@yandex.ru; bmat@iropt3.ioffe. rssi.ru; Mremennyy@mail.ioffe.ru).

Digital Object Identifier 10.1109/JSEN.2009.2033259

TABLE I
COMPARISON OF THE FIGURES OF MERIT FOR MODULATED THERMAL SOURCES AND LEDS FOR NDIR CO_2-SENSORS

Producer	Type	Optics	Consumed power, P_0, W	Modul. Freq., Hz	Emitter temp, ΔT^oC	Emitting power, P_E, mW	Active area cm^2	SWPE P_E/P_0, mW/W
Thermal sources (with spectral filter λ_{max} = 4.2 μm, $\Delta\lambda$ = 0.45 μm)								
HelioWorks	EP8520	Reflector	4.4	-	950	3.3		0.8
	EP3872	Reflector	2.4	2	1630	3.5		1.5
	EP8530		3.9	2	950	0.7		0.2
HawkEye Technology www.boselec.com	LC-IR-12		8.1	-	825	2.7	0.125	0.3
	CS-IR-20		4.0	-	825	1.1	0.0525	0.3
	IR-40		4.0	10	600	1.0	0.0875	0.3
	IR-55		0.9	10	750	0.27	0.0125	0.3
	IR-55 R	Reflector	0.9	10	750	2.7	0.0125	2.9
IonOptics (ICX Photonics)	NL8LNC		2.2	5	750	5.6	0.28	2.5
	Tun IR		0.135	1	750	0.27	0.09	2.0
Heimann Sensor www.heimannsensor.com	HSL EMIR-2000		0.45	10	450	0.18	0.0378	0.4
	HSL EMIR-2000R	Reflector	0.45	10	450	1.4	0.0378	3.1
Intex	MTRL-17-900		0.98	15	750	0.6	0.0289	0.6
	MTRL-17-900R	Reflector	0.98	15	750	3.8	0.0289	3.9
LEDs								
ICO Ltd (RMT) www.optico.ru	LED-42 λ_{max} = 4.1μm $\Delta\lambda$ = 0.8 μm		0.09 (80 mA*1.1V)	up to 10^5	<50	0.01		0.1
IoffeLed www.ioffeled.com Boston Electronics Corp. www.boselec.com	LED42Sc λ_{max} = 4.15μm $\Delta\lambda$ = 0.45 μm	Immers. lens	0.05 (200mA*0.25V)	up to 10^8	<50	0.03	0.09	1.5
Roithner	LED-43 λ_{max} = 4.3μm $\Delta\lambda$ = 1.0 μm	Reflector	0.075 (100mA*0.75V)	up to 10^8	<50	0.01		0.13

II. SOURCES AND DETECTORS OF RADIATION FOR NDIR GAS SENSORS

An optopair, i.e., a source and detector of radiation that are optically and spectrally matched, sometimes (usually when using thermal sources) with an additional narrowband spectral filter, is the most important part of the sensor. The most essential characteristics of optopairs are emitted and consumed power, operation speed, and detecting efficiency.

The present study considers the immersion "flip-chip" diodes developed at the Ioffe Institute as hardware components for sensors of optical gas analyzers. The choice is conditioned by the fact that at present, in our opinion, with respect to ensemble of technical characteristics they meet the requirements set to devices of wide-scale application to the fullest extent. Up-to-date ultra-compact thermal sources [7], [8] can be used as alternative sources of probing radiation in portable NDIR gas sensors. Table I presents principal characteristics of thermal sources and IR light-emitting diodes suitable for using in CO_2 sensors (CO_2 absorption line $\lambda_{\max} = 4.25\ \mu$m). Parameters of the emitted power (P_E) of sources were compared for the same values of a spectral band and angle of view specific for immersion lens diodes: $\Delta\lambda \approx 0.1\lambda_{\max} = 0.45\ \mu$m, output radiation pattern FWHM $\approx 30^\circ$. The spectral power of a wideband thermal source in a given spectral range and angle of view were estimated from the black body radiation law at the temperature recommended by fabricator with a coefficient equal to 0.7 that takes into account the emissivity of a material of a heating unit and spectral filter transmittance.

In order to compare the efficiency of using different sources, we have used the parameter spectral wall plug efficiency (SWPE) that is equal to the ratio of the emitted in a given spectral interval power (P_E) to the consumed power (P_0). The calculation show that the energetic efficiency of sources with additional optical elements (reflector, immersion lens) turns out to be approximately one and the same (of the order of fractions

TABLE II
COMPARISON OF THE FIGURES OF MERIT FOR PHOTORESISTORS, THERMOPILES, PYRODETECTORS, AND PHOTODIODES FOR NDIR CO_2-SENSORS

Producer	Type	Optics	Response time, s	NEP, nW/Hz$^{1/2}$	λmax /Δλ, mcm	Active/ Detection area, √A, cm	Detectivity, D*, cm Hz$^{1/2}$/W (295 K)
Photoresistors							
VIGO www.vigo.com.pl	PCI-4	Immers.lens	10^{-6}	$3.3\cdot10^{-3}$	up to 4	0.02/0.2	$6\cdot10^{9}$
	PC-4		10^{-6}	0.1	up to 4	0.2	$2\cdot10^{9}$
	PCI-5	Immers.lens	$0.5\cdot10^{-6}$	$5\cdot10^{-3}$	up to 5	0.02/0.2	$4\cdot10^{9}$
	PC-5		$0.5\cdot10^{-6}$	0.2	up to 5	0.2	$1\cdot10^{9}$
ICO Ltd www.optico.ru	PR1-38		$8\cdot10^{-6}$	0.04	up to 4.5	0.2	$5\cdot10^{9}$
	PR1-34		$30\cdot10^{-6}$	0.013	up to 4	0.2	$1.5\cdot10^{10}$
Thermopiles							
Heimann Sensors www.heimannsensor.com	HTS A11	sapphire	$6\cdot10^{-3}$	1.42	up to 5.5	0.08	$5.6\cdot10^{7}$
	HMS J11	sapphire	$6\cdot10^{-3}$	1.42	up to 5.5	0.08	$5.6\cdot10^{7}$
Pyrodetectors							
Heimann Sensors	HPSE09E		0.1	0.5	uniform	0.2	$4\cdot10^{8}$
Perkin Elmer	LHI807		0.1	0.9	uniform	0.15	$6.27\cdot10^{7}$
InfraTec	LM-395		0.15	0.45	uniform	0.2	$4.5\cdot10^{8}$
Photodiodes							
IoffeLed www.ioffeled.com	PD42Sc	Immers.lens	up to10^{-9}	$3\cdot10^{-3}$	4.15/0.45	0.03/0.33	$1\cdot10^{10}$
VIGO	PVI-4	Immers.lens	$15\cdot10^{-9}$	$5\cdot10^{-3}$	2.5-4	0.02/0.2	$4\cdot10^{9}$
	PV-4		$15\cdot10^{-9}$	0.1	2.5-4	0.1	$1\cdot10^{9}$
	PVI-5	Immers.lens	$15\cdot10^{-9}$	0.01	2.6-5	0.02/0.2	$2\cdot10^{9}$
	PV-5		$15\cdot10^{-9}$	0.2	2.6-5	0.1	$5\cdot10^{8}$

of percent) for thermal sources and LEDs at $\Delta\lambda = 0.45\ \mu$m. However, the thermal sources require greater by more than one order of magnitude values of applied power, which is caused by necessary heating of the emitting element up to temperatures equal to about 1000 K in order to shift the maximum of the spectral brightness of black body radiation to the mid IR range.

Moreover, so far, the thermal sources do not ensure the electrical modulation of radiation with frequencies above 10–15 Hz, which, in its turn, does not allow one to record the radiation beyond the frequency band of flicker noise that is an essential source of noise in measurement devices.

Thus, the high frequency of radiation modulation, possible operation without an additional interference filter and considerably less consumed and dissipated power are the main advantages of light-emitting diodes as compared to thermal sources.

Table II gives the main characteristics of present-day uncooled detectors of mid IR radiation, namely, photoresistors, thermopiles, pyrodetectors, and photodiodes. The spectral power of their basic noise (NEP) and operation speed are the principal parameters to be taken in order to perform the comparison of photodetectors. Similarly to the emitters, photodetectors supplied with immersion optics are characterized by the best parameters with respect to sensitivity and they permit decreasing self-noises up to the values equal to several picoWatt when detecting radiation of an area of several millimeters in diameter. The primary advantage of pyrodetectors is the uniformity of their spectral characteristics. At the same time, their low operation speed does not allow one to solve the above-noted problem of flicker-noise suppression and to create quick operating NDIR gas sensors. Thermopiles have a considerably shorter interval of response time (several milliseconds); however, their noises are greater than those of pyrodetectors by one order of magnitude. In fact, the detecting efficiency of present-day photoresistors is comparable with that of photodiodes at a chosen wavelength. However, the operation speed of photoresistors is less than that of photodiodes which can be as high as 10^8 Hz. Besides, unlike photoresistors, photodiodes can be used without additional reference voltage, which makes easier the solution of the problem of output signal stabilization and reduces the sensor energy consumption.

Thus, considering the total set of parameters, optopairs based on immersion light-emitting diodes and photodiodes are promising elements for the creation of efficient quick-operating NDIR gas sensors.

III. TRANSFER FUNCTION OF AN OPTICAL GAS SENSOR

Optical gas analyzers are spectral measurement devices whose operation is based on the well-known Beer–Lambert absorption law [8] relating the intensity of monochromatic radiation (λ) that has passed through a gas under study with

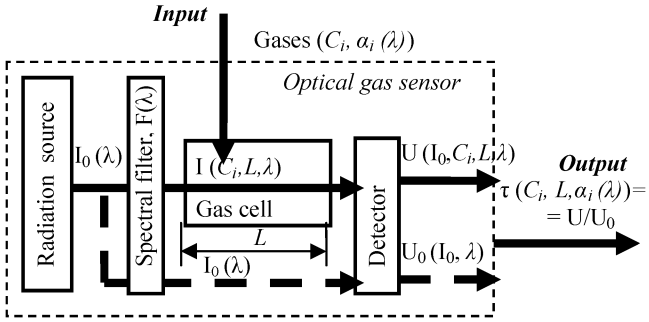

Fig. 1. Block diagram of an optical gas sensor.

concentration (C, v/v), absorption path length (L, cm) and gas spectral absorption coefficient $(\alpha(\lambda), \mathrm{cm}^{-1})$

$$I(C,\lambda) = I_0(\lambda) \cdot \exp\left[-\alpha(\lambda) \cdot L \cdot C\right]. \tag{1}$$

A device that performs the transformation of an input quantity C into a quantity to be measured $U(C,\lambda)$ is a measuring transducer. Its function in the optical gas analyzer is performed by an optical sensor whose structure diagram is shown in Fig. 1.

The optical sensor consists of a radiation source (sometimes with a narrowband spectral filter, $\mathrm{F}(\lambda)$) in order to form a probing beam $I_0(\lambda)$ in a given spectral interval, a volume with a gas under study (a gas cell) and detector of radiation. The gas under study attenuates the intensity of the probing radiation during its passing through the gas cell of length L. An electric signal $U(I_0, L, C, \lambda)$ depends on the intensity of the probing radiation $I_0(\lambda)$ and contains information on the gas concentration C is formed at the sensor output. It is clear that the parameter $I_0(\lambda)$ should be excluded in order to unambiguously determine the value C by the measured signal $U(I_0, L, C, \lambda)$. This condition may be fulfilled either by keeping the value $I_0(\lambda)$ at a certain (constant) level that is determined before the beginning of measurements or by introducing an additional "reference" channel in which a quantity proportional to $I_0(\lambda)$ is measured. There are different technical methods for excluding the influence of $I_0(\lambda)$ on measurement results; however, their analysis is out of the scope of the present study. Therefore, we shall consider the transmittance coefficient of the cell with gas as an output of the optical sensor

$$\begin{aligned}\tau\left(C, L, \alpha(\lambda)\right) &= \frac{I(C,L,\lambda)}{I_0(\lambda)} = \frac{U(C, I_0, L, \lambda)}{U_0(I_0, \lambda)} \\ &= \exp\left[-\alpha(\lambda) \cdot L \cdot C\right]. \end{aligned} \tag{2}$$

The transformation (2) that determines the functional dependence of the output quantity of an optical sensor on its input quantity, gas concentration C, is the transfer function of the sensor for the monochromatic probing radiation; it permits estimating the required gas concentration C at the gas sensor input by measuring the value $\tau(C, L, \lambda)$ at its output.

When using the probing source and detector of radiation with spectral characteristics overlapping a certain frequency band $\Delta\lambda = \lambda_2 - \lambda_1$, the photodetector measures an integral signal and the transfer function of the optical gas sensor takes into account spectral characteristics of sensor elements and "parasitic" absorption caused by the presence of foreign gases. It is described by the following integral expression (3) shown at the bottom of page, where

$R_{PhD}(\lambda, T)$	is the spectral sensitivity of a photodetector;
$P_E(\lambda, T)$	is the spectral power of a source of radiation;
$F(\lambda)$	is the spectral characteristic of a filter;
$\alpha(\lambda)$	is a spectrum of the absorption coefficient of a gas under study;
$\alpha_i(\lambda)$	are spectra of the absorption coefficients of foreign gases of concentrations C_i;
L	is the length of interaction of the probing radiation with the gas.

The temperature shift of spectral characteristics of a source and detector of radiation inherent to all semiconductor elements and photoresistors without exception leads to changes of the optical sensor output signal and, consequently, to errors in calculating the gas concentration. In order to take into account the effect of the sensor temperature on measured values of gas concentration in (3), we have introduced a temperature parameter T into the functions of spectral characteristics of a source $(P_S(\lambda, T))$ and detector $(R_{PhD}(\lambda, T))$ of radiation.

The product of spectral characteristics of the source and detector of radiation and spectral filter is an essential specific feature of an optopair used in a gas sensor. It determines the characteristics of the sensor as a spectral device and thus it can be considered as its *instrument function*

$$A\left(\lambda, \lambda_{\max}(T)\right) = R_{PhD} \cdot P_E(\lambda, T) \cdot F(\lambda). \tag{4}$$

So, different optopairs can be characterized completely by the instrument function with parameters $\lambda_{\max}(T)$ and $\Delta\lambda(T)$, whereas the transfer function will be written, as shown in (5) at the bottom of the next page.

$$\begin{aligned}\tau(C, L, T) &= \frac{U(C, L, T)}{U_0(T)} \\ &= \frac{\int_{\lambda 1}^{\lambda 2} R_{PhD}(\lambda, T) \cdot P_E(\lambda, T) \cdot F(\lambda) \cdot \exp\left[-\alpha(\lambda) LC\right] \cdot \prod_{1}^{N} \exp\left(-\alpha_i(\lambda) LC_i\right) d\lambda}{\int_{\lambda 1}^{\lambda 2} R_{PhD}(\lambda, T) \cdot P_E(\lambda, T) \cdot F(\lambda) d\lambda}\end{aligned} \tag{3}$$

The transfer function of an optical gas sensor $\tau(C)$ (5) is the principal functional dependence that allows one to estimate the sensor sensitivity within a total range of concentrations being measured, to compare different types of sensors with respect to sensitivity, and to estimate the attainable accuracy. The slope of the transfer characteristic $S(C) = d\tau/dC$ determines the *sensitivity of a sensor* that will be essentially different for different measurement ranges of concentration due to the nonlinearity of the transfer characteristic $\tau(C)$. In absolute terms the value of sensitivity is determined as $dC = d\tau/S(C)$. If we take that the minimum recorded change $d\tau$ is equal to $1/\Psi$ for a given signal-to-noise ratio (Ψ) of the sensor measurement circuit, then the *absolute error of measurements* and the related notion of the *limit of detection* (LOD) can be calculated by using the relationship

$$dC = \frac{1}{\Psi \cdot S(C)}$$
$$\mathrm{LOD} = \frac{1}{\Psi \cdot S(C \to 0)}. \tag{6}$$

Thus, the description of the NDIR gas sensor as a spectral measurement device with the help of instrument (4) and transfer (5) functions permits solving such important practical problems originating when developing measurement techniques as the determination of measurement error value with changing environmental temperature and/or determination of the range of operational temperatures for which this error does not exceed a given value. Besides, it allows one to determine the sensitivity and accuracy of measurements within different ranges of concentration measurements.

IV. Transfer Function of an Optical Gas Sensor Based on Immersion Optopairs

In order to carry out a mathematically precise description of functional dependence (5), it is necessary to know the analytical expressions for spectral characteristics of absorption coefficients of a gas under study, radiation source, photodetector, and their temperature dependencies.

A. Spectral Distribution of a Gas Absorption Coefficient

Radiating (absorbing) ability of gas molecules in the IR spectrum range is caused by vibration rotational mechanism of oscillations of molecules and it has a clearly expressed ruled structure. In this case, gas absorption bands consist of a great number of spectral lines that are spaced practically uniformly apart, their width being determined by the probability of collisions between gas molecules. Under standard measurement conditions (STP), the half-width of these lines (FWHW) is equal to about 0.1 cm^{-1} (less than 10^{-3} μm) and the spectral line shape is roughly described by the Lorentzian that determines the radiation (absorption) coefficient for each spectral component [10]

$$k_i(\lambda) = \frac{S(\lambda_i)}{\pi} \cdot \frac{\sigma_L}{\sigma_L^2 + \left(\frac{1}{\lambda} - \frac{1}{\lambda_i}\right)^2} \tag{7}$$

where the line intensity is

$$S(\lambda_i) = \int_0^\infty k_i(\lambda) d\lambda.$$

Each spectral line is described by three main parameters:

- Resonance wavelength λ_i [cm] that does not depend either on pressure or gas temperature (up to the states of a strongly rarefied gas).
- Intensity $S(\lambda_i)$ $[\mathrm{cm}^{-1}/(\mathrm{molecule}\cdot\mathrm{cm}^{-2})]$. The line intensity $S(\lambda_i)$ does not depend on pressure and its temperature dependence may be calculated from the energy value of the "low" state E'' $[\mathrm{cm}^{-1}]$, λ_i and temperature dependences of rotational (Q_R) and vibration (Q_V) distribution functions.
- Line width σ_L $[\mathrm{cm}^{-1}/\mathrm{atm}]$ that has a certain temperature dependence; in a general case, σ_L is proportional to $(T/T_s)^{-1/2}$, where $T_s = 296$ K corresponds to STP.

In order to find the value of absorption of probing radiation during its passing through a gas, the spectral absorption coefficients $(\alpha(\lambda), \mathrm{cm}^{-1})$ are used. We have applied the analytical model of spectral distribution of gas absorption coefficients calculated from the tables of line intensity of gas radiation $S(\lambda_i)$ in a given spectral range that meets the following approximations:

- Spectrum of a gas absorption coefficient is described by the sum of Lorentz distributions with different λ_i and $S(\lambda_i)$ and equal values of σ_L, which is primarily depends on the nature and pressure of the background gas

$$\alpha(\lambda) = \sum_i \frac{S(\lambda_i)}{\pi} \cdot \frac{\sigma_L}{\sigma_L^2 + \left(\frac{1}{\lambda} - \frac{1}{\lambda_i}\right)^2}. \tag{8}$$

  Characterization of sL under STP and decision-making its fitting criterion were the primary tasks of optical gas sensors simulation.
- Spectra of absorption coefficients of all gases are given within a spectral band 3–5 μm (2000–3350 cm^{-1}) with the spacing of 0.01 nm. The fulfillment of this condition is necessary for a joint analysis of radiance sources, detectors, gas mixtures and study the influence of temperature and foreign gases.
- The simulation takes into account only the lines with intensity $S(\lambda_i) \geq 0.1\ \mathrm{cm}^{-1}/(\mathrm{molecule}\cdot\mathrm{cm}^{-2})$ under STP.

When developing mathematical models, one of the principal points is the choice of a check criterion for their validity. Experimental gas absorption spectra from the Pacific Northwest

$$\tau(C, L, T) = \frac{\int_{\lambda 1}^{\lambda 2} A\left(\lambda, \lambda_{\max}(T)\right) \cdot \exp\left[-\alpha(\lambda) \cdot L \cdot C\right] \cdot \prod_1^N \exp\left(-\alpha_i(\lambda) \cdot L \cdot C_i\right) d\lambda}{\int_{\lambda 1}^{\lambda 2} A\left(\lambda, \lambda_{\max}(T)\right) d\lambda} \tag{5}$$

National Laboratory (PNNL) database [11] have been taken as reference spectra for checking the validity of the model being developed. The spectra were recorded with the help of a Fourier spectrometer with the resolution equal to 0.1 cm^{-1} within the range 6500–600 cm^{-1} and gas concentration equal to $C = 1\ \mathrm{ppm}$ at an absorption wavelength $L = 1\ \mathrm{m}$.

We have used the tables of the electronic edition [12] of the international database HITRAN (high resolution transmission molecular absorption database) for setting the parameters λ_i and $S(\lambda_i)$. The value σ_L was evaluated by trial-and-error method from the coincidence of gas absorption spectra calculated in accordance with our model and experimental spectra from the data of the PNNL laboratory. Good matching of the carbon dioxide absorption spectra calculated by using the proposed model and PNNL experimental spectra has been obtained at $\sigma_L = 0.085\ \mathrm{cm}^{-1}/\mathrm{atm}$ (about 0.15 nm/atm). The validity of this value for CO_2 spectrum of absorption coefficient is confirmed not only by the good matching with PNNL data, but also by our sequel testing of $CO_2 + N_2$ mixtures at different CO_2 concentrations.

B. Spectral Characteristics of Immersion Light-Emitting Diodes and Photodiodes

As it was mentioned in Section III, the instrument function of a sensor is one of its main characteristics that is determined by spectral characteristics of sensor elements. Therefore much attention in the present research has been paid to experimental studies of spectral characteristics of immersion lens light-emitting diodes and photodiodes, to their temperature dependence and possible analytical description. As can be seen from Tables I and II, immersion light-emitting diodes and photodiodes are relatively narrowband, which permits one to use them without additional interference filters and to set $\mathrm{F}(\lambda) = 1$ in expression (4) for a sensor instrument function.

Other properties of the immersion lens diodes include a small angle of view, certain dependence of the spectral characteristic on the angle of acquisition of radiation determined by the geometry of a lens and existence of chromatic aberrations in it, and a relatively narrow spectral band ($\Delta\lambda/\lambda \approx 0.1$–$0.15$). The last property is caused by spectral filtering of radiation with a lens material and layers through which the input of radiation into a diode active region is performed. In this case, there is a sharp decay of the sensitivity spectrum in the long-wavelength part caused by a decrease of the absorption coefficient of a semiconductor material at $h\nu < E_g$ and a sharp decay in the short-wavelength part that generally coincides with the transmission spectrum of the substrate or the set substrate-optical glue-lens.

Fig. 2 demonstrates typical spectral characteristics of conventional light-emitting diodes of type LED42Sc [Fig. 2(a)] and photodiodes of type PD42Sc [Fig. 2(b)] (that are unadjusted with respect to the system transmission) together with approximating Lorentz distribution functions $L(\lambda_{\max}, \Delta\lambda)$ for LED and sum of Gauss distributions $G(\lambda_{\max}, \Delta\lambda)$ for photodiodes

$$P_{LED}(\lambda, T) = \frac{P_0}{\pi} \cdot \frac{\Delta\lambda(T)}{\Delta\lambda(T)^2 + (\lambda - \lambda_{\max}(T))^2}$$
$$R_{PD}(\lambda, T) = R_0 \cdot [k_1 \cdot G1\,(\lambda_{\max}(T), \Delta\lambda(T)) + k_2 \cdot G2\,(\lambda_{\max}(T) - \lambda_{sh}, \Delta\lambda_{sh})] \quad (9)$$

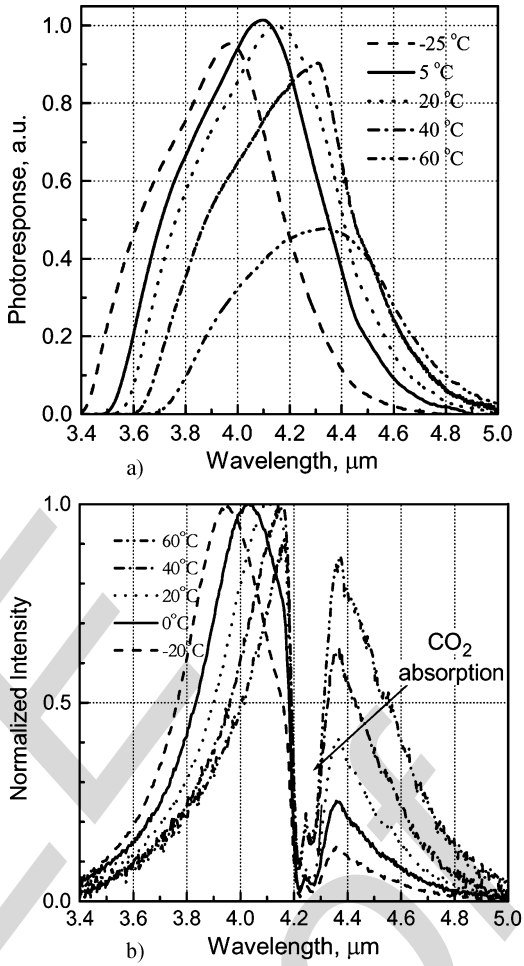

Fig. 2. (a) Experimental spectral characteristics of light emitting diodes LED42Sc and (b) photodiodes PD42Sc at different operational temperatures.

where λ_{sh} and $\Delta\lambda_{sh}$ are parameters, uniquely defined for photodiodes of different types. For PD42Sc $\lambda_{sh} = 0.35\ \mu\mathrm{m}$ and $\Delta\lambda_{sh} = 0.2\ \mu\mathrm{m}$.

One can see the dips in Fig. 2(b) that are related to the presence of absorption by carbon dioxide containing in the air (concentration C is equal to about 0.03 vol. %, $L \approx 1\ \mathrm{m}$) in the range 4.25 μm. The position of the maximum of spectral lines ($\lambda_{\max}$) obeys the linear law with a shift temperature coefficient 4.2 nm/degree, that is one and the same for LEDs and photodiodes. In order to estimate the half-width of the radiation spectral line within the temperature interval 20 °C–50 °C, one may use an approximate expression $\Delta\lambda(T) \approx k \cdot \lambda_{\max}(T)$. The relationship $\Delta\lambda(T)$ becomes nonlinear with the temperature range extension, however, its behavior remains being one and the same for LED and photodiodes.

As can be seen from Fig. 2, the spectral lines for photodiodes turn out to be slightly wider than those for LEDs. This difference is explained, first of all, by the fact that the high energy radiation (beyond the fundamental absorption edge) is absorbed efficiently in a photodiode and it contributes into the photocurrent under certain conditions. On the contrary, in a light-emitting diode, the probability of photon emitting with energy higher than the band gap energy decreases exponentially with quanta

energy increase, and the LED emission spectrum is always relatively narrow.

The photosensitivity spectrum of the flip-chip photodiodes under consideration (i.e., they are illuminated from a substrate side) appear to be considerably narrower than that for the case of conventional photodiodes that are illuminated from a p-n junction side. The diffusion length of carriers in photodiodes illuminated from the substrate side turns out to be much less than the thickness of a substrate and layers through which photoinduced carriers could reach the region of the p-n junction volume charge due to diffusion and cause photocurrent/photo-e.m.f. As a result, the short wavelength edge of the photosensitivity of such photodiodes is determined mainly by the optical transmittance of intermediate layers and substrate that is related in a number of cases to the degree of substrate doping and can be chosen according to a problem to be solved. For example, when using highly doped substrates n+—InAs(Sn) with electron degeneracy in the conductivity band, the InAsSb photodiode photosensitivity spectrum spreads from 3 up to 4.55 μm [12].

In the present work, InAsSb photodiodes ($\lambda_{\max} = 4.3\ \mu\mathrm{m}$) have been studied on a substrate n—InAs ($n = 2E16\ \mathrm{cm}^{-3}$). As can be seen from Fig. 2(b), the short wave edge of the photosensitivity of these photodiodes is situated in the region 3.75μm, which leads to their high selectivity. This corresponds best to the problem of creation of one-channel gas analyzers.

One of specific features of the flip-chip structure is the fact that light-emitting diodes and photodiodes are fabricated from identical semiconductor structures. In this case, the temperature dependence identity of spectral characteristics of light-emitting diodes and photodiodes permit one to state that the shape of the instrument function of an optical gas sensor based on immersion optopairs does not change with temperature and different optopairs can be described by the instrument function with the unique parameter $\lambda_{\max}(T)$.

C. Optopair Instrument Function. Transfer Function of a Carbon Dioxide Gas Sensor

From expression (5) at $\sigma_L = 0.085\ \mathrm{cm}^{-1}$, the values λ_i and $S(\lambda_i)$ for carbon dioxide given in [11] and spectral characteristics of light-emitting diodes and photodiodes (9), the instrument and transfer functions of a specific specimen of a carbon dioxide gas sensor based on immersion LED42Sc ($\lambda_{\max}(20\ ^\circ\mathrm{C}) = 4.11\ \mu\mathrm{m}$) and PD42Sc ($\lambda_{\max}(20\ ^\circ\mathrm{C}) = 4.08\ \mu\mathrm{m}$) have been calculated, which enables obtaining the optopair resulting instrument function with $\lambda_{\max}(20\ ^\circ\mathrm{C}) = 4.10\ \mu\mathrm{m}$ that is shown in Fig. 3(a) together with the CO_2 transmission spectrum. As can be seen from Fig. 3(a), the change of the sensor temperature leads to considerable mismatching of the instrument function and envelope contour of the carbon dioxide spectrum.

Fig. 3(b) and (c) demonstrate the results of calculations of optical sensor transfer functions with cell lengths equal to 0.25 and 4 cm within a temperature interval 0 °C–45 °C for the above-considered optopair. As can be seen, the optopair parameter $\lambda_{\max}(T)$ effects considerably the width of the uncertainty band of the sensor transfer function caused by the temperature shift of its instrument function.

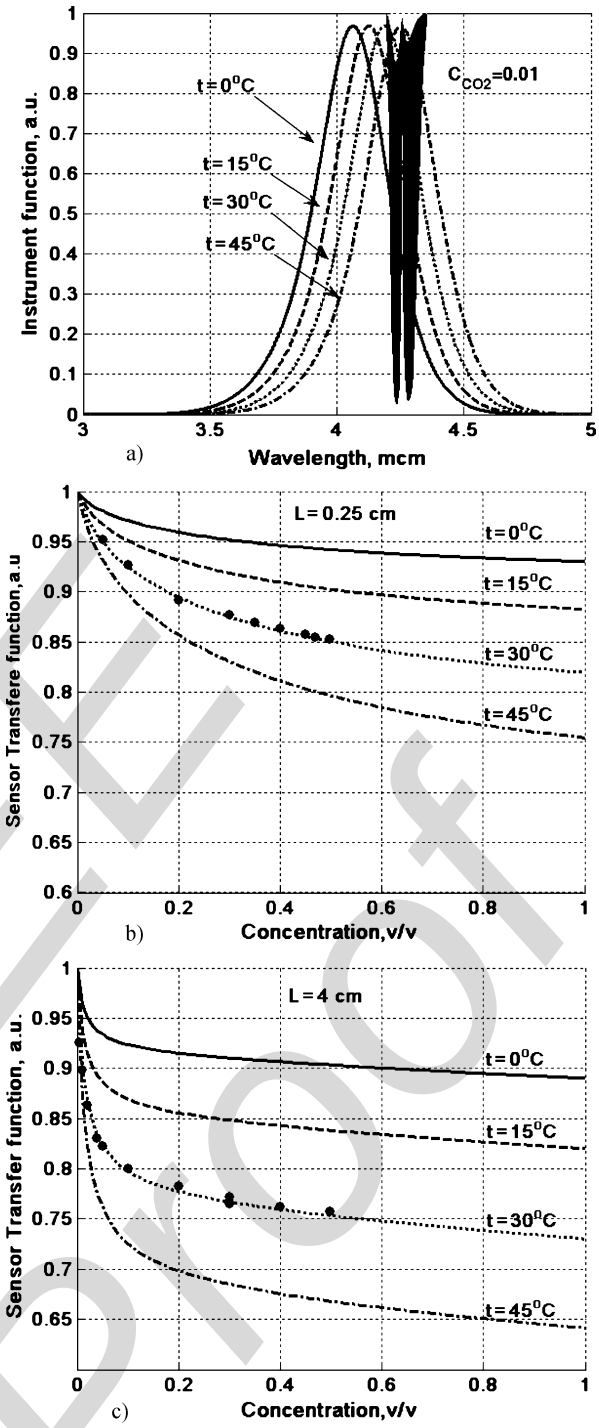

Fig. 3. CO_2 transmission spectrum for CL $= 1$, instrument (a) and transfer (b), (c) functions of a CO_2-sensor with (b) $L = 0.25$ cm and (c) $L = 4$ cm for an optopair with $\lambda_{\max} = 4.1\ \mu\mathrm{m}$ at different operational temperatures.

D. Experimental Studies of the Transfer Function of a Carbon Dioxide Sensor

A laboratory model of a pocket-size optical sensor of carbon dioxide based on the above-considered optopair using the light-emitting diode LED42Sc and photodiode PD42Sc was fabricated and its characteristics were studied in order to check the validity of the chosen approach. The model provided the possibility to change the length of the gas cell and sensor

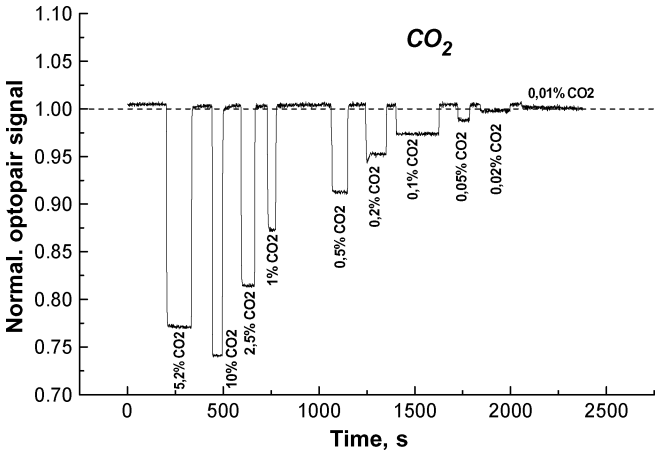

Fig. 4. Output signal of the CO_2-sensor model for $L = 4$ cm.

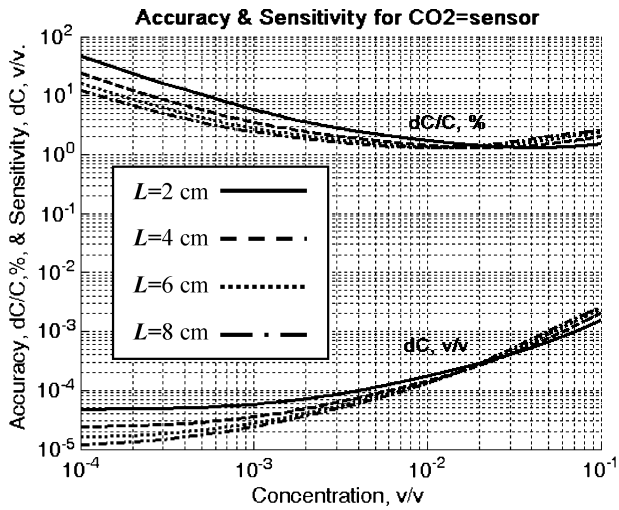

Fig. 5. Sensitivity and accuracy of measurements for the CO_2-sensor based on the immersion lens diode optopair with the instrument function with $\lambda_{\max}(20°C) = 4,\ 1\ \mu$m for the gas cell length $L = 2 \ldots 8$ cm and $\Psi = 3000$.

temperature, digitization and transfer of current values of optopair signals along the channel RS 232 for subsequent computer processing. The sensor operational speed that is determined by the low-frequency filter parameters in the circuit of photodetector signal processing was equal to 100 ms (10 readings per second). The sensor gas cell represented a tube of the inner diameter equal to 3 mm (corresponding to the immersion lens diameter), which provides a small volume of a gas sampling under analysis, i.e., equal to about 0.2 ml, and widens essentially potential application fields of the sensor. At small sensor sizes ($L = 0.25$–10 cm), the viewing angle of immersion optics $\leq 30°$ permits one to obtain without additional optical elements the level of the signal-to-noise ratio Ψ at the output of circuits of photodetector signal detecting and processing equal to $(5 - 10) \cdot 10^3$ at the chosen operational speed. The model has been fabricated with using a light-emitting diode operating in the meandre mode (duty cycle 50%) with the pulse-repetition rate equal to 20 kHz at an average current equal to 200 mA. The light-emitting diode LED42Sc is characterized by $\lambda_{\max}(20\ °\mathrm{C}) = 4.11\ \mu$m and the immersion photodiode PD42Sc used as a detector is characterized by $\lambda_{\max}(20\ °\mathrm{C}) = 4.08\ \mu$m, which provides the resulting instrument function of the optopair with $\lambda_{\max}(20\ °\mathrm{C}) = 4.10\ \mu$m that is shown in the right part of Fig. 3(a).

The model was tested with using calibration CO_2 and N_2 mixtures for carbon dioxide concentrations within the range 0.01–50 v/v %). After each measurement, nitrogen purging of the system has been accomplished for "zero calibration" performance. Fig. 4 shows the form of the output signal in case the gas cell length $L = 4$ cm and the count frequency is equal to $10\ s^{-1}$ (the experimentally recorded signal-to-noise ratio is equal to 1000). The sensor model temperature after 30-min heating settled constant and was equal to 33 ± 1 °C during the experiment.

In Fig. 3(b) and (c), the points are for the experimental transfer function values of the gas analyzer laboratory model with the gas cell length $L = 0.25$ cm (b) and $L = 4$ cm (c) for carbon dioxide of different concentration. A good coincidence of the calculated and experimental data can be seen within a wide range of carbon dioxide concentrations. The discrepancy of the data does not exceed 0.5%, which indicates the validity of the proposed model.

The criterion of accuracy of any measurements is the value of relative error of the obtained result ($\delta = dC/C$). Fig. 5 demonstrates the expected values of the sensitivity (absolute error) and accuracy (relative error) of measurements for a sensor whose instrument function is characterized by $\lambda_{\max}(20\ °\mathrm{C}) = 4.1\ \mu$m at different lengths of the gas cell and for the experimentally obtained value $\Psi = 3000$ of the signal-to-noise ratio of the measurement circuit in case the response time was equal to 1 s. The calculations were made for the sensor temperature equal to 300 °C.

The signal-to-noise ratio $\Psi > 3000$ is securely obtained at the output of the gas sensor model due to high efficiency of using the radiation energy of immersion diodes. The plots in Fig. 5 show that in the range of CO_2 concentrations up to 0.1–10 v/v %, the measurement absolute error does not exceed 1%–2%. The limit of detection of the sensor under consideration becomes less than 0.0025 v/v % (25 ppm) for $L \geq 4$ cm, which is the peak value for pocket-size (the volume of the gas cell is less than 1 ml) portable gas analyzers for a given operational speed.

V. Comparison of the Sensitivity of CO_2-Sensors With Different Hardware Components

The CO_2-sensor transfer function calculated for a sensor based on immersion lens light-emitting diodes and photodiodes with instrument functions presented in Fig. 3(a) can be used for estimating the sensitivity of sensors with different hardware components. It proceeds from the fact that CO_2-sensors with equal instrument functions are described by the same transfer characteristic that does not depend on the used hardware components. When using wideband sources and detectors of radiation, narrowband spectral filters are usually used, and the sensor instrument function is determined by the filter characteristic. Since the interference filter typical shape is close to the instrument function of an immersion diode optopair that we have obtained, we may compare the sensitivity of CO_2-sensors fabricated with using different hardware components by applying the results given in the previous section.

TABLE III
COMPARISON OF THE SENSITIVITY OF CO_2-SENSORS WITH DIFFERENT HARDWARE

CO_2-Optopair configuration ($\lambda_{max} \approx 4.2$ μm)	**Normalized signal-to-noise ratio $\xi_P = \Psi/(P_0 \cdot \sqrt{t}) = P_E/(P_0 \cdot NEP)$, $\sqrt{Hz}/W$**	**Optopair time constant, s**	**Normalized LOD, (ppm·cm)/(mW•√s)**
Thermal source + Photoresistors	$\sim 1 \cdot 10^9$	0.1	0.3
Thermal source + Thermopiles	$2 \cdot 10^6$	0.1	160
Thermal source + Pyrodetectors	$(2\text{-}6) \cdot 10^6$	0.1	50…..160
Thermal source + Photodiodes	$0.5 \cdot 10^9$	0.1	0.7
LED + Photoresistors	$0.5 \cdot 10^9$	10^{-6}	$2 \cdot 10^{-3}$
LED + Thermopiles	$1.0 \cdot 10^6$	10^{-2}	100
LED + Pyrodetectors	$2.8 \cdot 10^6$	0.1	100
LED + Photodiodes	$0.2 \cdot 10^9$	10^{-8}	$0.5 \cdot 10^{-3}$

As can be seen from expressions (6), in case the transfer function is the same, the signal-to-noise ratio value Ψ that is ensured by optopair elements is fundamental when estimating the parameters of sensor sensitivity. Therefore, let us consider the capabilities of CO_2-sensors based on different hardware components with respect to the sensitivity by evaluating the limiting values of Ψ from the parameters of the elements given in Tables I and II.

In order to compare the efficiency of optopairs with different hardware components, let us introduce a parameter of 'normalized signal-to-noise ratio' $\xi_P = P_E/(P_0 \cdot \mathrm{NEP}) = \Psi/(P_0 \cdot \sqrt{t})$, $[\sqrt{\mathrm{Hz}}/\mathrm{W}]$ determining the value Ψ that can be achieved in the optopair under consideration during unit of time per unit of power applied to the radiation source. The second column of Table III shows the values ξ_P calculated by the data from Tables I and II for the best parameters of their elements. The evaluated data of ξ_P (Table III, column 2) demonstrate that the efficiency of the optopairs based on thermal sources+photoresistor, on thermal sources+photodiode, on light-emitting diode+photoresistor, and on light-emitting diode+photodiode is high and practically the same. In order to estimate the expected limit of detection, one can introduce a normalized LOD whose dimensionality is $\mathrm{ppm}/(\mathrm{mW} \bullet \sqrt{\mathrm{s}})$. It allows us to estimate the limiting sensitivity of a sensor for the measurement time interval equal to 1 s and the power applied to the source of radiation equal to 1 mW. These values are shown in the last column of Table III; they indicate the considerable advantage of applying immersion light-emitting diodes and photodiodes, i.e., the achievement of high sensitivity (the lowest normalized LOD)—less than $10^{-3}\ \mathrm{ppm/mW} \cdot \sqrt{\mathrm{s}}$ at the minimum energy consumption-less than 0.05 mW (Table I, column 7).

VI. MAIN RESULTS AND CONSLUSION

Immersion lens mid infrared light-emitting diodes and photodiodes are the most advanced elements for the creation of NDIR gas sensors.

The analytical description of a NDIR gas sensor has been suggested with the aim to determine sensor instrument and transfer functions for estimating its main parameters as a measurement device. Such approach permitted us to produce the analytical model of the NDIR gas sensor that serves as a base for expert evaluations when comparing sensors with different hardware components and when solving applied problems of designing of different-purpose optical gas analyzers.

The study presents the model of a CO_2-sensor based on immersion diode optopairs. The calculated values of the threshold sensitivity at the level equal to tens of ppm, sensitivity not less than 0.1 vol.% and measurement accuracy at the level 1%–2% within the range 0–10 v/v % CO_2 for the operational speed up to 10 readings per second and gas cell length $L = 4\,\mathrm{cm}$ exceed the parameters of present-day produced CO_2-sensors. The known pocket-size high-speed sensors that are used mainly in capnography have the sensitivity in the low-concentration range (up to 5 v/v % CO_2) not less than 0.25 v/v % and relative accuracy of reading not less than 5% when measuring CO_2 concentrations higher than 5 v/v % [14]–[16].

The experimental results of the study of the carbon dioxide sensor model confirm the validity of the model and fair prospects for using the sensors based on immersion diode optopairs in portable gas analyzers.

REFERENCES

[1] S. D. Smith, H. R. Hardaway, and J. D. Crowder, "Recent developments in the applications of mid-infrared lasers, LEDs and other solid state sources to gas detections," in *Proc. SPIE*, 2002, vol. 4651, pp. 157–172.

[2] M. A. Remennyi, N. V. Zotova, S. A. Karandashev, B. A. Matveev, N. M. Stus', and G. N. Talalakin, "Low voltage episide down bonded mid-IR diode optopairs for gas sensing in the 3.3–4.3 mcm spectral range," *Sensors & Actuators B: Chemical*, vol. 91, no. 1–3, pp. 256–261, 2003.

[3] B. A. Matveev, "LED-photodiode opto-pairs," in *Mid-Infrared Semiconductor Optoelectronics*, ser. Springer Series in OPTICAL SCIENCE. : , 2006, pp. 395–428, 0342-4111.

[4] M. A. Remennyy, B. A. Matveev, N. V. Zotova, S. A. Karandashev, N. M. Stus, and N. D. Ilinskaya, "InAs and InAs(Sb)(P) (3–5 μm) immersion lens photodiodes for portable optic sensors," in *SPIE Proceedings*, F. Baldini, J. Homola, R. A. Lieberman, and M. Miler, Eds., May 2007, vol. 6585, Optical Sensing Technology and Applications.

[5] in *Concertation Meeting—FP7 Photonics Projects Barcelona*, Spain, September 18–19, 2008 [Online]. Available: http://cordis.europa.eu/fp7/ict/photonics/concertation180908_en.html

[6] G. Y. Sotnikova, S. A. Aleksandrov, G. A. Gavrilov, A. A. Kapralov, B. A. Matveev, and M. A. Remennyy, "Modeling of performance of mid-infrared gas sensors based on immersion lens diode optopairs," in *Proc. 7-th IEEEE SENSORS-2008*, Lecce, Italy, Oct. 2008, pp. 278–281.

[7] HawkEye Technologies [Online]. Available: www.hawkeyetechnologies.com

[8] J. Hildenbrand, A. Kurzinger, C. Peter, E. Moretton, J. Wollenstein, F. Numann, M. Ebert, and J. Korvic, "Micromachined mid-infrared emitter for fast transient temperature operation for optical gas sensing system," in *Proc. 7-th IEEEE SENSORS-2008*, Lecce, Italy, Oct. 2008, pp. 297–300.
[9] G. S. Landsberg, *Optics*. Moscow: Nauka Publishing House, 1976, p. 567.
[10] S. W. Share and T. J. Jonson *et al.*, "Gas-phase databases for quantative infrared spectroscopy," *Applied Spectroscopy*, vol. 58, no. 12, pp. 1452–1460, 2004.
[11] Pacific Northwest National Laboratory [Online]. Available: http://www.nwir.pnl.gov
[12] High Resolution Transmission Molecular Absorption Database (HITRAN'2008 Database, Version 13.0) [Online]. Available: http://www.cfa.harvard.edu
[13] A. L. Zakhgeim, N. V. Zotova, N. D. Il'inskaya, B. A. Matveev, M. A. Remennyi, N. M. Stus', and A. E. Chernyakov, "Room-temperature broadband InAsSb flip-chip photodiodes with $\lambda_{\text{cut off}} = 4.5\ \mu\text{m}$," *Semiconductors*, vol. 43, no. 3, pp. 394–399, 2009.
[14] COMET CO2_1,2 CardioPulmonary Technologies, Inc [Online]. Available: www.treymed.com
[15] Microstream Capnography Module [Online]. Available: www.oridion.com
[16] CO_2 Detector Nonin Medical, Inc [Online]. Available: www.nonin.com

Galina Yu. Sotnikova graduated with a Degree from the Leningrad Politechnical Institute (now-Politechnical University), St. Petersburg, Russia, in 1980. She received the Ph.D. degree in radiophysics from the Politechnical Institute, in 1987. Her Ph.D. work was devoted to optoelectronic signal processing based on CCD image sensors.

She joined the Ioffe Physical-Technical Institute in 1987, where she is a Senior Scientific Researcher at the Solid-State Electronic Department, Ioffe Institute. She is an author of more than 40 papers and 4 patents, project manager of a number of research projects: Foundation for Assistance to Small Innovative Enterprises (grants #4269p/4719, 2004–2008, Innovation Development grant of the Russian Academy of Sciences, 2007). Her current scientific interests include the analysis and mathematic simulation of optical signal detection and communication technique.

Gennadyy A. Gavrilov graduated with a degree from the V. I. Ulyanov (Lenin) Electrical Engineering Institute ("LETI"), ***[location]***, in 1961. In the same year he joined the Ioffe Physical-Technical Institute, St. Petersburg, Russia, and received the Ph.D. degree in experimental physics in 1967. His Ph.D. work was devoted to problems of registration of optical images.

Now, he is a Senior Scientific Researcher at the Solid-State Electronic Department, Ioffe Physical-Technical Institute RAS. He is an author of more than 100 papers and 4 patents. He is the scientific leader of the Optoelectronics Group, Laboratory of Holography and Optoelectronics. His current interests relate to the optoelectronic information processing technique and equipment.

Sergey E. Aleksandrov graduated with a Degree from Politechnical University, St. Petersburg, Russia, in 1997. He is preparing the Ph.D. thesis devoted to the infrared gas and temperature sensors.

In 1997, he joined the Solid-State Electronic Department, Ioffe Physical-Technical Institute as a Scientific Researcher. His current interests relate to the microchip hardware and software for optoelectronic control and measuring devices. He is a Project Manager of research projects of the Foundation for Assistance to Small Innovative Enterprises (grant #5761p/8178, 2008–2009).

Alexander A. Kapralov graduated with a Degree from the Politechnical University, St. Petersburg, Russia, in 1997.

Since 1997, he has been a Scientific Researcher at the Solid-State Electronic Department, Ioffe Physical-Technical Institute RAS. His current interests relate to the microchip hardware and software for optoelectronic control and measuring devices.

Sergey A. Karandashev graduated with a Degree from the Electrical Engineering Institute ("LETI"), ***[location]***, in 1982.

He is a Scientific Researcher at the Ioffe Physical-Technical Institute, St. Petersburg, Russia. His research interests include the investigation of electroluminescence and optical properties of narrowband A3B5 alloys and mid-IR LEDs and photodiodes.

Boris A. Matveev graduated with a Degree from the V. I. Ulyanov (Lenin) Electrical Engineering Institute ("LETI"), ***[location]***, in 1977. At the same year he joined the Ioffe Institute. His Ph.D. work (1987) was devoted to the investigation of deformation in narrow gap III–V semiconductor heterostructures.

He is a Senior Researcher at the Ioffe Physical-Technical Institute, Centre of Nanoheterostructure Physics, St. Petersburg, Russia. His current interests relate to investigation of mid-IR LEDs and detectors for optoelectronic IR analyzers. He is an author of more than 100 papers and 5 patents and a scientific leader of the Middle Diode Optopair Group (MIRDOG) involved in domestic and international research programs: CRDF grants #807, #1261(3), #1483 (1999–2005), Foundation for Assistance to Small Innovative Enterprises (grants #5982, #06-2-H4.2-0201), Ministry of Sciences of the RF (3 grants), 2001–2005.

Prof. Matveev received awards including the Ioffe Institute Prize for the Best Work in 2001, and the Frenkel Premium for the Best Work at the Ioffe Insttitute, 2007.

Maxim A. Remennyy graduated with a Degree from St. Petersburg Technical University, St. Petersburg, Russia, in 1995 and received the Ph.D. degree in semiconductor physics from the Ioffe Institute, St. Petersburg, in 1999.

He is senior Scientific Researcher at the Ioffe Physical-Technical Institute. Now, he works on mid-IR diode lasers, noncooled LEDs and photodiodes. He has personal national research grants for young scientists: "Mid-IR (3–5 μm) Negative and Positive Luminescence Sources from InAs Based Solid Solution with microstructured surface" (No MK-1804.2005.02), "Vertically emitting InAs/InAsSbP DH LEDs and lasers for the 3–4 μm spectral range" (grant No PD04-1.2-259, «Mid-IR (3–5 μm) Negative Luminescent A3B5 Based Devices with Built-in Cavities» (No MK-1597.2003.02), "Development and investigation of powerful mid-IR LEDs (3–4 μm) with two dimentional photonic crystals and internal radiation concentration for chemical sensors" (FASIE-UMNIK, 2007).